Performance Analysis, Real Time Simulation and Control of Medium-Scale Commercial Aircraft Turbofan Engine

Chang Duk Kong*
Department of Aerospace Engineering, Chosun University
Jayoung Ki
Department of Mechanical Engineering, Chosun University
Suk Chou Chung
Department of Mechanical Design Engineering, Seoul National Polytechnic University

The turbofan engine performance analysis for a medium scale commercial aircraft was carried out and the LQR control scheme for performance optimization was studied. By using scaled component maps from well-known CF6 engine characteristics, the steady-state performance analysis result was compared with BR715-56 engine performance data. The transient performance analysis was performed with four fuel schedules. The linear simulation was done at the maximum take-off condition. The real time linear simulation was performed by interpolation of the system matrices, which used the least square method as the function of LPC rotational speed. By using linear system matrices of design point, the LQR controller which used control variables for the fuel flow and the LPC bleed air was designed.

Key Words : Performance Analysis, Real Time Simulation, Optimal Control, Turbofan Engine

Nomenclature

BLEED : %Bleed air from compressor
C_p : Specific heat coefficient
FN : Net thrust
h : Enthalpy
I : Moment of inertia
$\dot{m}$: Air mass flow rate
N : Rotational speed
P : Pressure
$PCNF$: Fan rotor %RPM
$PCNC$: High pressure compressor %RPM
PR : Pressure ratio
SM : Surge margin
TIT : Turbine inlet temperature
TFF : Turbine flow function
U : Internal energy
WFB : Fuel mass flow Rate
$XNLP$: Low pressure rotor speed
$XNHP$: High pressure rotor speed
η : Efficiency

Subscripts

a : Air
$D.$: Design point
g : Gas
M : Map point
$M.D.$: Map design point
HPC : High pressure compressor
HPT : High pressure turbine
LPC : Low pressure compressor
LPT : Low pressure turbine
$1, 2;\cdots, 7$: Component station number
mL : Low pressure turbine mechanical loss
mH : High pressure turbine mechanical loss
tot : Total

* Corresponding Author,
E-mail : cdgong@mail.chosun.ac.kr
TEL : +82-62-230-7188; **FAX** : +82-62-232-9218
DepartmentofAerospaceEngineering,ChosunUniversity, #375 Seosuk-dong, Kwangju 501-600, Korea.(Manuscript **Received** October 2, 2000 ; **Revised** February 5, 2001)

1. Introduction

The turbofan engine is being used for medium or large scale commercial aircraft recently due to

Table 1 Comparison of BR715-56 engine performance data, design point analysis result, and steady-state performance analysis results

	BR715-56 Data	Design Point	Steady-state Performance Analysis			Unit
			Take-off	Climb	Cruise	
Mach No.	0	0	0	0.78	0.78	
Altitude	0	0	0	35,000	39,000	ft
Temperature Amb.	ISA+27	ISA+27	ISA+27	ISA+18	ISA	°R
Pressure Amb.	14.644	14.644	14.644	5.086	4.198	Psi
Air Flow Rate	598.2	598.2	598.2	239.99	191.05	Lb/sec
LPC PR	1.673	1.673	1.673	1.743	1.645	
Booster PR	1.19	1.19	19.25	19.554	18.836	
HPC PR	15.97	15.97				
HP TIT	2943	2943	2943	2763	2464.2	°R
Bypass Ratio	4.67	4.67	4.669	4.716	4.776	
Thrust	19,696	19,605.68	19,671.05	4,325.48	3,058.98	lbf
SFC	0.375	0.375	0.363	0.6314	0.5964	lb/hr/lbf

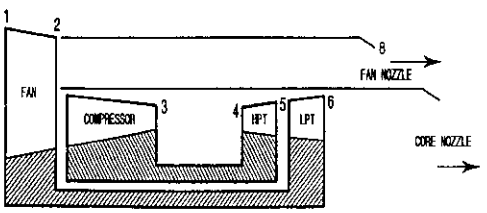

Fig. 1 Station No. of turbofan engine for performance analysis

its advantages of little noise and lower specific fuel consumption relatively. It was selected for the suitable engine of a medium scale aircraft, which had been conceptually developed in Republic of Korea.

The optimal control scheme has been needed to improve the performance of the engine and the control technique has been developed with performance improvement of a personal computer. Therefore the performance of the engine depends on how the controller is optimal, concern about the engine controller is being increased. To design the most optimal controller, real time linear simulation must be preceded.

The exact engine performance simulation is essential for reasonable prediction of performance, safe operation, and the life usage as well as diagnostics of a engine. It has been developed to find the best way to reduce the developing cost and risk due to various experiments (Sellers et al., 1975; Pilidis, 1996).

The simulation of aero engines with nonlinear characteristics has been derived for actual engine performance modification or engine design in the preliminary design phase. The dynamic simulation program, which is available to predict the dynamic performance, has been continuously developed (Sellers et al., 1975 ; Fawke et al., 1971 ; Schobeiri et al., 1994).

Moreover, the application of the modern control scheme might be required. When the precise model is obtained, it is possible to design the optimal controller, which has been considered by designers(Geyser, 1978; Bettocchi et al., 1996).

Various types of controller were designed with the purpose of system characteristics. It has been designed using a trial and error method in optimal conditions (Mahmoud et al., 1991; Watts et al., 1992).

In this study, the station number of turbofan engine for a performance analysis is shown as Fig. 1.

The turbofan engine performance for a medium scale commercial aircraft was analyzed and the control scheme to improve the performance was studied.

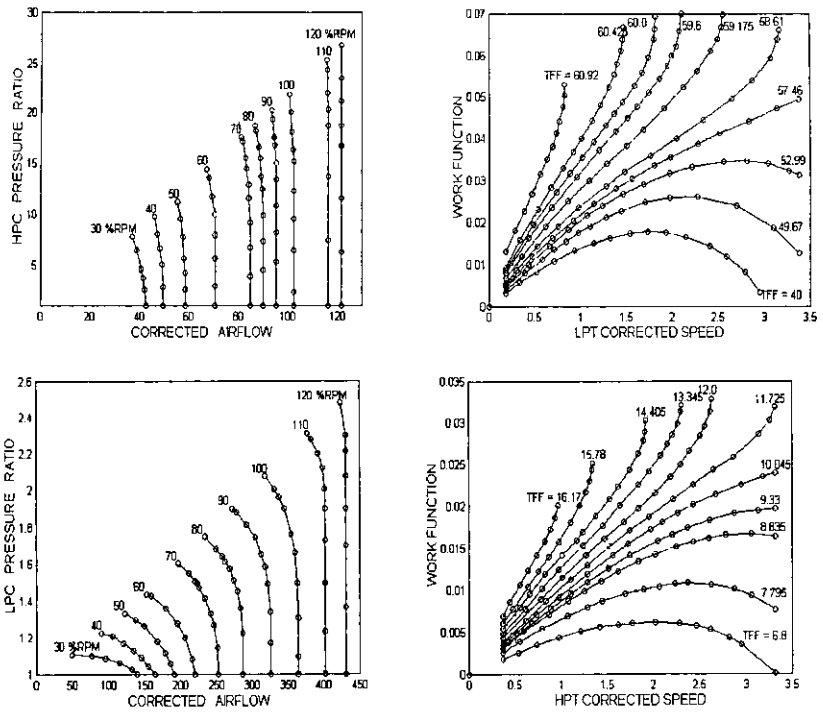

Fig. 2 Scaled turbofan engine component characteristics

2. Steady-State Performance Analysis

In general the design point is determined by the performance requirement condition of an engine. By using the engine performance data of BR715-56 engine, the design point was selected, and the component map was scaled from the well-known CF6 engine.

The engine performance is analyzed by both the steady-state performance analysis and the transient performance analysis considering various engines operating condition. In this study the design point performance analysis was carried out at the maximum take off condition and the off design point performance analysis was performed at the maximum climb and at a cruise condition.

For steady-state performance analysis, performance matching between components based on flow and energy conservation laws is required. Therefore, the following conditions (Cohen et al., 1996) are assumed.

1) The rotational speed of the compressor and turbine connected with the same shaft must be the same.

2) The airflow passed through each component, must be constant.

3) The work done by the compressor and the turbine connected with the same shaft must be the same.

The performance of each component follows the scaled performance characteristics from the original characteristics.

Each component's performance curve of BR 715-56 engine decided as a medium scale aircraft turbofan engine has not been published yet because it is the property of an engine manufacturer. Therefore, it was obtained by scaling the performance curve of the well-known CF6 engine as Fig. 2, in predicting components' performance of BR715-56 engine. The scaling laws used in this study were as follows (Sellers et al., 1975; Pilidis, 1996);

$$PR=\frac{PR_D-1}{PR_{MD}-1}(PR_M-1)+1 \tag{1}$$

$$\dot{m}=\frac{\dot{m}_D}{\dot{m}_{MD}}\dot{m}_M \tag{2}$$

$$\eta=\frac{\eta_D}{\eta_{MD}}\eta_M \tag{3}$$

The closer scaling factor is 1.0, and the simulated maps of the engine are more reasonable for larger value.

2.1 Design point performance analysis

Two methods of the design point analysis, which were the cycle analysis and the steady-state performance analysis by using the component performance characteristics obtained by scaling, were carried out at the maximum take off condition of BR715-56 engine. The result was compared with the BR715-56 engine data.

The compressor of BR715-56 engine is composed of the low-pressure compressor , the booster and the high pressure compressor. In order to simplify the performance analysis, the turbofan engine model which was composed of the low-pressure compressor without booster and the high-pressure compressor was used. In the steady-state performance analysis result with the scaled component characteristics, the bypass ratio was almost the same as the BR715-56 data, the error of the thrust and the specific fuel consumption were 0.12% and 3.2%, respectively. The comparison of BR715-56 engine performance data with the design point cycle analysis result and the steady-state performance analysis results was shown in Table 1.

2.2 Off design point performance analysis

Off design points mean all operating ranges of engine excluding the design point. The off design point performance analysis must be carried out to predict the engine performance at all operating ranges.

For the steady-state performance analysis, matching of the rotational speed, airflow, and the work between compressors and turbines were required as follows.

• Rotational speed compatibility equation

$$\frac{N_{LPT}}{\sqrt{T_5}}=\frac{N_{LPC}}{\sqrt{T_1}}\times\sqrt{\frac{T_1}{T_5}}$$

$$\frac{N_{HPT}}{\sqrt{T_4}}=\frac{N_{HPC}}{\sqrt{T_2}}\times\sqrt{\frac{T_2}{T_4}} \tag{4}$$

• The flow compatibility equations

$$\frac{\dot{m}_{HPC}\sqrt{T_2}}{P_2}=\frac{\dot{m}_{tot}\sqrt{T_1}}{P_1}-\frac{\dot{m}_{fan}\sqrt{T_{21}}}{P_{21}}$$

$$\frac{\dot{m}_{HPT}\sqrt{T_4}}{P_4}=\frac{\dot{m}_{HPC}\sqrt{T_2}}{P_2}\times\frac{P_2}{P_3}\times\frac{P_3}{P_4}\times\sqrt{\frac{T_4}{T_2}}$$

$$\frac{\dot{m}_{LPT}\sqrt{T_5}}{P_5}=\frac{\dot{m}_{HPT}\sqrt{T_4}}{P_4}\times\frac{P_4}{P_5}\times\sqrt{\frac{T_5}{T_4}}$$

$$\frac{\dot{m}_{NOZZLE}\sqrt{T_6}}{P_6}=\frac{\dot{m}_{LPT}\sqrt{T_5}}{P_0}\times\frac{P_5}{P_6}\times\sqrt{\frac{T_6}{T_5}} \tag{5}$$

• The work compatibility equations

$$\eta_{mL}C_{pg}\Delta T_{56}=C_{pa}\Delta T_{12}$$

$$\eta_{mH}C_{pg}\Delta T_{45}=C_{pa}\Delta T_{23} \tag{6}$$

Through the result of the off design performance analysis with above compatibility equations, it was found that the analysis results were very similar to the BR715-56 performance data as the high pressure compressor turbine inlet temperature was $1535K$ at the maximum climb condition and $1369K$ at the cruise condition. It showed that the bypass ratio differences were 7.18% and 0.76%, the power thrust differences were 2.47% and 3.69%, and the specific fuel consumption differences were 6.32% and 8.1% respectively.

2.3 Partload performance analysis

The part load performance analysis was carried out with 5% interval rpm of low pressure compressor from 70% to 100% rpm at three flight conditions (maximum take-off, maximum climb and cruise) selected as the design and the off design points. The result is shown in Fig. 3. At three flight conditions, the fuel flow, the thrust and the HPT inlet temperature were increased linearly with rotational speed increase and the specific fuel consumption was decreased within LPC 90% RPM and increased after then. When the LPC rotational speed was 90% RPM at each flight condition, the specific fuel consumption showed the best performance.

3. Transient Performance Analysis

When fuel input is rapidly increased or de-

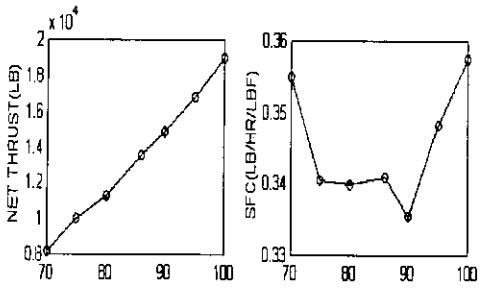

Fig. 3(a) Partload performance at maximum take-off condition

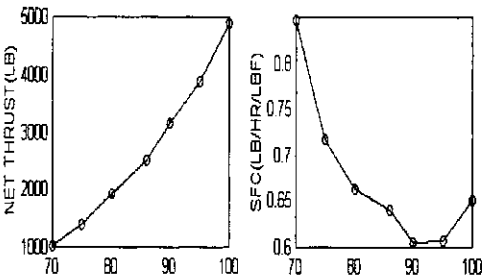

Fig. 3(b) Partload performance at maximum climb condition

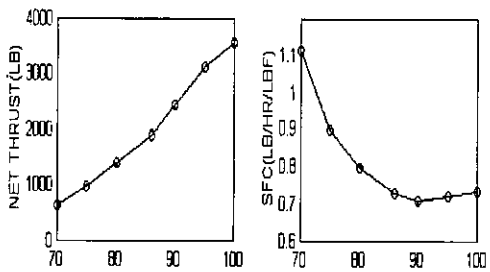

Fig. 3(c) Partload performance at cruise condition

creased, the engine is in a transient state. In the transient state, work of the same spool with compressor and turbine is surpassed or insufficient. Therefore, it would not be suitable for the required work balance between the compressors and the turbines. Consequently, the engine is frequently beyond the operational range, which may damage the engine or shorten its lifetime. Above all, when the engine is operated during rapid acceleration, the overshoots of the turbine inlet temperatures exceed the limit temperature, and the compressor surges occurs. It can cause structural damage by excessive thermal stress produced in the turbine blade, and unstable operation by the compressor surges.

Therefore, it is very important that the dynamic characteristics of the engine should be simulated correctly or anticipated to Improve the reliability of the engine.

The work differences between the compressors and the turbines in the transient state can be expressed as the following equation (Sellers et al., 1975).

$$\dot{m}_{LPT}\Delta h_{LPC}=\dot{m}_{LPC}\Delta h_{LPC}+\left(\frac{2\pi}{60}\right)^2\left(\frac{dN}{dt}\right)\text{IN}$$

$$\dot{m}\Delta h_{HPT}=\dot{m}_{HPC}\Delta h_{HPC}+\left(\frac{2\pi}{60}\right)^2\left(\frac{dN}{dt}\right)\text{IN} \tag{7}$$

For performance analysis of the transient state, the rotational speed increase or decrease is calculated by integrating the surplus torque of the second term of the right hand side equation. In this study, the Euler method was used for integration.

Fuel mass flow required for changing the low pressure compressor from idle RPM to maximum rotational speed has been changed by four cases which were step increase, ramp increase, ramp decrease and ramp decrease after step increase, and also the dynamic simulation of the major variables has been observed. Here, the overshoot occurred at the high-pressure compressor turbine inlet temperature due to the variation of fuel mass flow as Fig. 4. For maximum climb condition of the case that the fuel mass flow was increased in step or in ramp with the time rate within 4.5 seconds, it was found that the compressor stall had happened at the high-pressure compressor. Therefore, to eliminate this the fuel mass flow must be increased in ramp with time interval over than 5.5 seconds and it has been confirmed that the high-pressure compressor turbine inlet temperature exceeded the limit temperature (e.g. BR715-56 engine case is 1725K), and then the overshoot occurred. Therefore the damage can be given rise to the high pressure at compressor turbine blade.

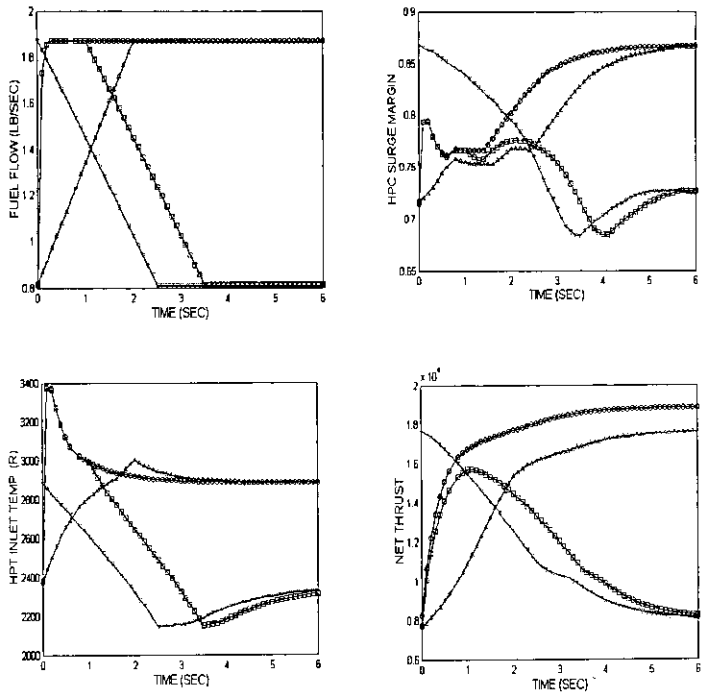

Fig. 4(a) Transient performance analysis at maximum take-off condition. (-○-: Step inc', -△-: Ramp inc', -▽-: Ramp dec', --: Step inc' & Ramp dec')

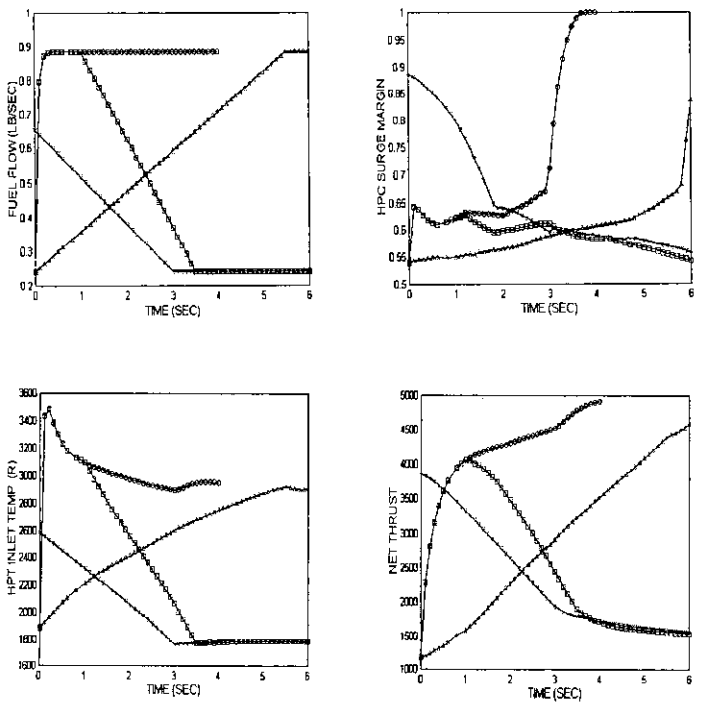

Fig. 4(b) Transient performance analysis at maximum climb condition (-○-: Step inc', -△-: Ramp inc', -▽-: Ramp dec', --: Step inc' & Ramp dec')

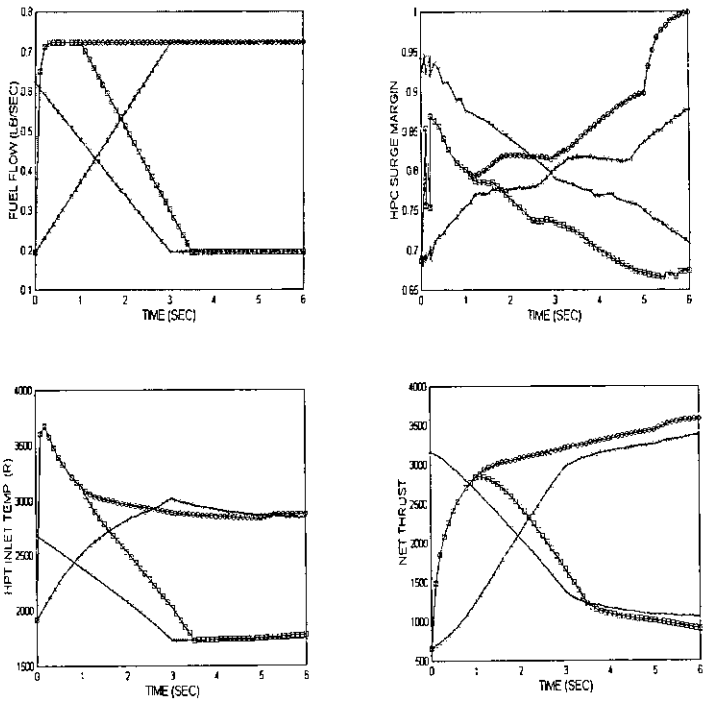

Fig. 4(c) Transient performance analysis at cruise condition. (-○-: Step inc', -△-: Ramp inc', -▽-: Ramp dec', --: Step inc' & Ramp dec')

4. Real-Time Linear Simulation

To apply the modern control scheme, linearization of a nonlinear engine might be required.

A nonlinear time invariant system is expressed as follows;

$$\text{State equation : } \dot{x}=f(x,\ u) \tag{8}$$

$$\text{Output equation : } y=g(x,\ u) \tag{9}$$

Where $x\in R_n$, $y\in R_m$, and $u\in R_r$ respectively.

Expanding Eqs. (8) and (9) about an arbitrary operating point(x_s, u_s) with the Taylor expansion series, and neglecting over second-order terms, the nonlinear system can be expressed by the following linearized state equation;

$$\delta\dot{x}=A\delta x+B\delta u$$
$$\delta y=C\delta x \tag{10}$$

where $\delta x=x-x_s$, $\delta\dot{x}=\dot{x}-\dot{x_s}$, $\delta y=y-y_s$, $\delta u=u-u_s$, $y_s=g(x_s,\ u_s)$, and $\dot{x_s}=f(x_s,\ u_s)$ respectively.

Using DYGABCD, the A, B, C matrices were obtained for the partial difference of 1% on each operating point (Geyser, 1978).

The state space equation has state variables such as rotor speeds, compressor outlet pressures, and turbine inlet temperatures. The fuel flow rate and the bleed air were control input, and the rotor speeds, the compressor surge margins, the HPT inlet temperatures, the thrust and the specific fuel consumption were output variables.

Therefore,

$\delta x=[\delta$XNLP, δXNHP, δP2, δP3, δU4, δU5, δU6$]^T$

$\delta u=[\delta$WFB, δBLEED$]^T$

$\delta y=[\delta$PCNF, δPCNC, δLPCSM, δHPCSM, δTIT, δFN, δSFC$]^T$

Because of the state variable change with rotor speeds, matrices of state space equations must be changed due to rotor speed change (Kerr et al. 1992; Mihaloew et al. 1984; Smith et al. 1990). In the real time linear simulation, first of all, scheduled sampling data were needed. To minimize errors and calculation time, proper

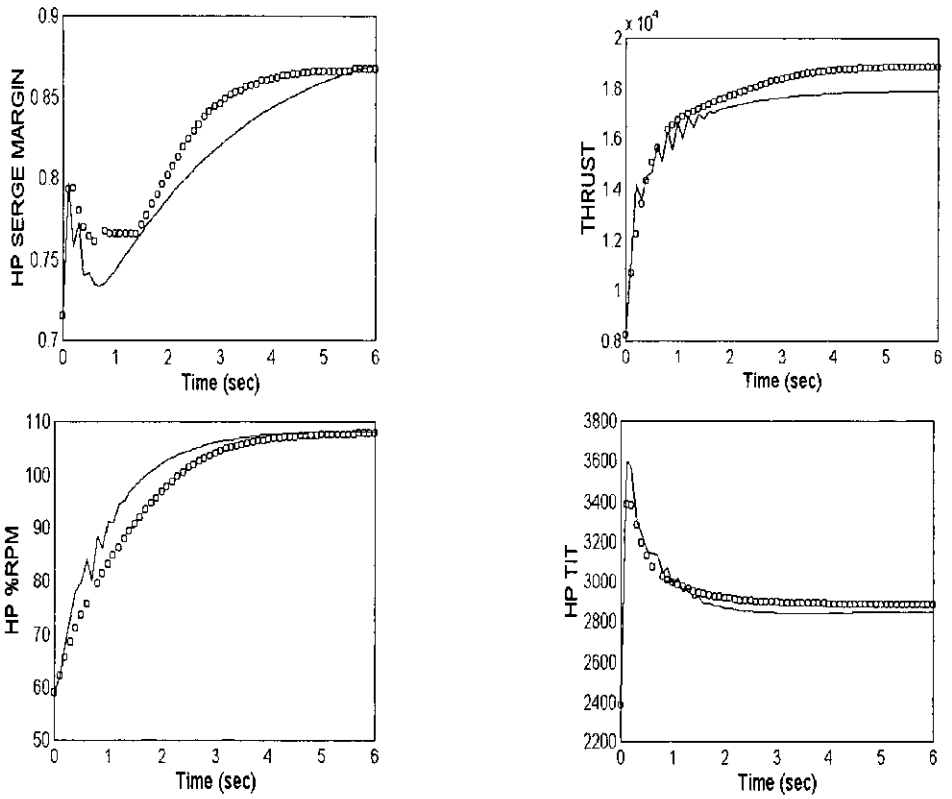

Fig. 5 Comparison of nonlinear simulation and real-time linear simulation at maximum take-off condition (○ ○ ○: Nonlinear, --------: Linear).

sampling data were needed. The 5% interval from LPC 70% RPM to 100% RPM linear models and the real time piecewise linear model in maximum take-off condition were considered.

Firstly, in operating points x_i (i=0, 1, 2, ⋯ , n), if the approximate function $p(x)$ and the original function $f(x)$ are in the following relation;

$$f_i=f(x_i)-\mathrm{P}(x_i),\ (i=0,\ 1,\ 2,\ \cdots,n) \quad (11)$$

The least square method is to be least square of f_i. Then

$$\sum_{i=0}^{n} f_i^2=\sum_{i=0}^{n}[f(x_i)-p(x_i)]^2 \quad (12)$$

In this study, from the comparison of the real time linear model with a fifth-order polynomial as a function of LPC rotational speed and nonlinear simulation, the steady state error of main performance variables was within 8% so that it could be enough to be acceptable. The comparison result was shown as Fig. 5.

5. Optimal LQR Controller

The optimal linear quadratic regulator (LQR), which has been widely used as a modern control scheme, was developed by Kalman in 1960 (Merrill et al. 1984 ; Garg , 1996).

The cost function J to determine the optimal control $u(0)$ is defined as follows;

$$J=\int_0^\infty (x^TQx+u^TRu)dt \quad (13)$$

Where Q is a real symmetric n by n positive semi definite matrix. And R is a real symmetric m by m positive definite matrix.

If the optimal control is unique and all states are observable, the optimal control law yields as follows;

$$u=-Gx=R^{-1}B^TKx \quad (14)$$

Table 2 Control weighted matrix R, state weighted matrix Q, and control gain K for LQR controller in maximum take-off condition.

$$R=\begin{bmatrix} 4800 & 0 \\ 0 & 80000 \end{bmatrix}$$

$$Q_1=\begin{bmatrix} 1/2700 & 0 & 0 & 0 & 0 & 0 & 0 \\ 0 & 1/2700 & 0 & 0 & 0 & 0 & 0 \\ 0 & 0 & 1/2700 & 0 & 0 & 0 & 0 \\ 0 & 0 & 0 & 1/2700 & 0 & 0 & 0 \\ 0 & 0 & 0 & 0 & 1/2700 & 0 & 0 \\ 0 & 0 & 0 & 0 & 0 & 1/2700 & 0 \\ 0 & 0 & 0 & 0 & 0 & 0 & 1/2700 \end{bmatrix}$$

$$Q_2=\begin{bmatrix} 1/600000 & 0 & 0 & 0 & 0 & 0 & 0 \\ 0 & 1/600000 & 0 & 0 & 0 & 0 & 0 \\ 0 & 0 & 1/600000 & 0 & 0 & 0 & 0 \\ 0 & 0 & 0 & 1/600000 & 0 & 0 & 0 \\ 0 & 0 & 0 & 0 & 1/600000 & 0 & 0 \\ 0 & 0 & 0 & 0 & 0 & 1/600000 & 0 \\ 0 & 0 & 0 & 0 & 0 & 0 & 1/600000 \end{bmatrix}$$

$$G_1=\begin{bmatrix} 0.0002 & 0.0000 & -0.0003 & 0.0013 & 0.0000 & 0.0000 & 0.0000 \\ 0.0000 & 0.0000 & 0.0000 & 0.0000 & 0.0000 & 0.0000 & 0.0000 \end{bmatrix}$$

$$G_2=1.0E-005\times\begin{bmatrix} 0.1158 & -0.0137 & -0.2032 & 0.9303 & 0.0250 & -0.0002 & 0.0000 \\ 0.0008 & 0.0001 & 0.0002 & 0.0078 & 0.0001 & 0.00000 & .0000 & 0.0000 \end{bmatrix}$$

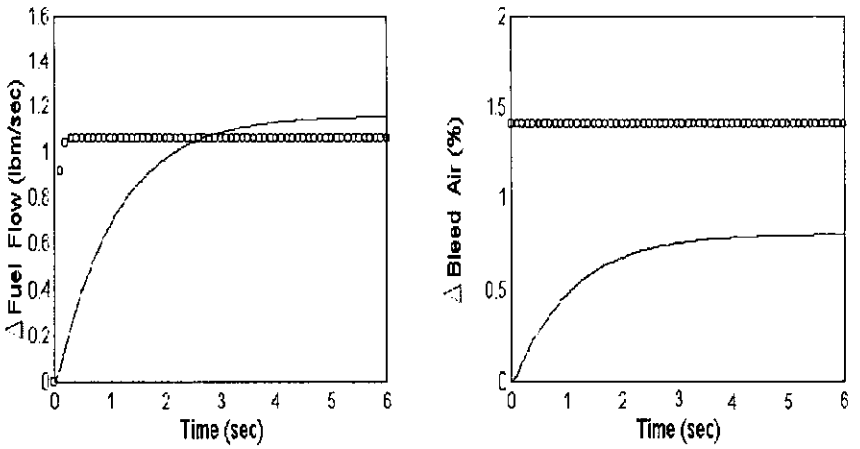

Fig. 6 Comparison of control input variables between nonlinear simulation and LQR controller at maximum take-off condition. (○ ○ ○: Nonlinear, --------: LQR)

where K is the positive semi definite matrix and unique solution for the following equation.

$$0=KA+A^TK+Q-KBR^{-1}B^TK \quad (15)$$

Therefore, in order to design a LQR controller, the selection using the trial and error method of the control weighted matrix R, the state weighted matrices Q, and the control gain G were obtained by MATLAB as Table 2 (Kong et al. 1997; Frederick et al. 1995; Kong et al. 1999).

5.1 Controller design result

The controller design result was compared with the nonlinear dynamic simulation result as Figs. 6 and 7.

Table 3 Comparison for results between nonlinear simulation and LQR controller

Variable		S-S Time	S-S Value	Unit
WFB	Nonlinear Simulation	0.5sec	1.8739	lb_m/sec
	LQR Control	5.3sec	1.8953	
Bleed Air	Nonlinear Simulation	·	1.4	%
	LQR Control	4.5sec	0.8	
HP %RPM	Nonlinear Simulation	5.8sec	107.8	%
	LQR Control	4.8sec	112	
Max. HPC SM	Nonlinear Simulation	4.6sec	0.867	
	LQR Control	5.5sec	0.58	
HPT TIT	Nonlinear Simulation	4.8sec	2886.38	°R
	LQR Control	3.3sec	2900.00	
FN	Nonlinear Simulation	6sec	18864	lb_f
	LQR Control	6sec	18810	
SFC	Nonlinear Simulation	·	0.583	lb_m/lb_f-hr
	LQR Control	·	0.43	

The compared performance variables are two control variable and the HPC %RPM, the HPC surge margin, the HPT inlet temperature, and the thrust. The maximum HPC surge margins, steady-state values for each variable, and settling time were followed as Table 3.

In applying the fuel step increase case in the maximum take-off condition, the nonlinear and real-time linear models had an overshoot of HPT inlet temperature. Therefore, the LQR controller was designed to eliminate the overshoot of HPT inlet temperature.

The fuel step increase case to 1.8739lbm/sec in maximum take-off condition has shown that the HPC %RPM response of the LQR controller was 4.8 seconds, and the steady-state error of the controller was 4.2%. In attempting to control the overshoot of HPT inlet temperature, the settling time of the LQR controller was 3.3 seconds, which was faster than 4.8 seconds of the nonlinear model. The steady state errors of the LQR controller were 0.47%. The overshoot of HPT inlet temperature was effectively eliminated by the LQR controller as Fig. 7.

The fuel flow rate of the LQR controller was increased slower than the nonlinear simulation. However the controlled bleed air was less than the nonlinear simulation as 0.8%, and the controlled HPC surge margin was larger than the nonlinear simulation as 0.55~0.75.

6. Conclusions

The steady-state and transient performance analysis, the real-time linear simulation, and controller design for medium scale commercial aircraft turbofan engine were performed.

(1) The steady-state performance analysis of BR715-56 engine was compared with the study engine performance to verify the analysis method.

(2) The result of the partload performance analysis has shown that the specific fuel consumption of the best performance was around the LPC 90%RPM.

(3) In the transient performance analysis, the HPT inlet temperature exceeded the limit temperature at all flight conditions in the cases of step fuel increase and ramp fuel increase, and the surge occurred in the HPC at the maximum climb condition in the cases of step fuel increase and ramp fuel increase up to 4.5 seconds.

(4) The LQR controller was designed, controlled to eliminate effectively HPT inlet temperature overshoot and obtain enough HPC surge margin for the safe operation.

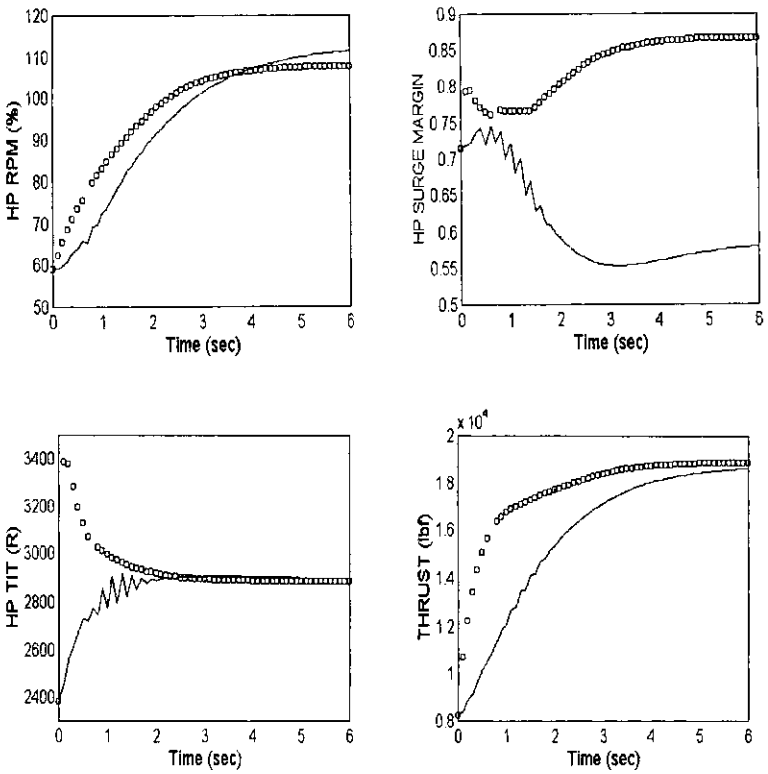

Fig. 7 Comparison of output variables between nonlinear simulation and LQR controller at maximum take-off condition.(○ ○ ○: Nonlinear, --------: LQR)

Acknowledgement

This study was supported by research funds from Chosun University, 2000.

References

Bettocchi, R., Spina, P. R., and Fabbri, F., 1996, "Dynamic Modeling of Single-Shaft Industrial Gas Turbine," *ASME 96-GT-332*.

Cohen, H., Rogers, G.F. C., and Saravanamuttoo, H. I. H., 1996, "Gas Turbine Theory," *Longman*, 4th Ed.

Cranfield Univ., 1996, "Gas Turbine Performance," *Cranfield Short Course Note*, UK.

Fawke, A.J., Saravanamuttoo, H. I. H., 1971, "Experimental Investigation of Methods for Improving the Dynamic Response of a Twin-Spool Turbojet Engine," *J. of Eng. for Power*, pp. 418~424.

Frederick, D.K. and Chow, J. H., 1995, "Feedback Control Problem - Using MATLAB and the Control System Toolbox," *PWS Publishing Co.*

Garg, S., 1996, "A Simplified Scheme for Scheduling Multivariable Controllers and Its Application to a Turbofan Engine," *ASME 96-GT-104.*

Geyser, L. C., 1978, "DYGABCD - A Program for Calculating Linaer A, B, C, D Matrices from a Nonlinear Dynamic Engine Simulation," *NASA TP 1295.*

Kerr, L.J., Nemec, T.S., and Gallops, G.W., 1992, "Real Time Estimation of Gas Turbine Damage Using a Control-Based Kalman Filter Algorithm," *J. of Eng. for Gas Turbines and Power*, Vol. 114, pp. 187~195.

Kong, C.D, Koh, k., and Ki, J., 1999, "Performance Analysis, Real Time simulation and Optimal Control of Medium-Scale Commercial Aircraft Turbofan Engine," *ISABE99-7101, 14th ISOABE Conference.*

Kong, C.D., Ki, J., and Koh, K., 1999, " Steady-State and Transient Performance Simulation of a Turboshaft Engine with Free Poowe Turbine," *ASME 99-GT-375*.

Kong, C.D., Kim, S.K., 1997, "Real Time Linear Simulation and Control for the Small Aircraft Turbojet Engine," *ASME 97-AA-114*.

Kong, C.D., and Chung, S.J., 1999, "Real Time Linear Simulation and Control for Small Aircraft Turbojet Engine," *KSME International J.*, Vol13, No. 9, PP. 656~666.

Mahmoud, S., McLean, D., 1991, "Effective Optimal Control of an Aircraft Engine," *Aeronautical Journal*, pp. 21~27

Merrill, M., Lehtinen, B., and Zeller, J., 1984, "The Role of Modern Control Theory in the Design of Control for Aircraft Turbine Engines," *J. of Guidance*, Vol. 7, No. 6, pp. 652~661.

Mihaloew, J. R., Roth, S. P., and Creekmore, R., 1984, "Real Time Pegasus Propulsion System Model V/STOL-Piloted Simulation Evaluation," *J. of Guidance*, Vol. 7, No. 1, pp. 77~84.

Schobeiri, M.T., Attia, M., and Lippke, C., 1994, "GETRAN : A Generic, Modularly Structured Computer Code for Simulation of Dynamic Behavior of Aero and Power Generation Gas Turbine Engines," *J. of Gas Turbines and Power*, Vol. 116, pp. 483~494.

Sellers, J.F., Daniele, C.J., 1975, "DYNGEN-A Program for Calculating Steady-State and Transient Performance of Turbojet and Turbofan Engine," *NASA TN D-7901*.

Smith, D.L., Stammetti, V.A., 1990, "Sequential Linearization as an Approach to Real-Time Marine Gas turbine Simulation," *J. of Eng. For Gas Turbines and Power*, Vol. 112, pp. 187~191.

Watts, J.W., Dwan, T.E., Brockus, C. G., 1992, "Optimal State-Space Control of a Gas Turbine Engine," *J. of Eng. for Gas Turbine and Power*, Vol. 114, pp. 763~767.